Bradycardia and Slowing of the Atrioventricular Conduction in Mice Lacking $Ca_V3.1/\alpha_{1G}$ T-Type Calcium Channels

Matteo E. Mangoni,* Achraf Traboulsie,* Anne-Laure Leoni, Brigitte Couette, Laurine Marger, Khai Le Quang, Elodie Kupfer, Anne Cohen-Solal, José Vilar, Hee-Sup Shin, Denis Escande, Flavien Charpentier, Joël Nargeot, Philippe Lory

Abstract—The generation of the mammalian heartbeat is a complex and vital function requiring multiple and coordinated ionic channel activities. The functional role of low-voltage activated (LVA) T-type calcium channels in the pacemaker activity of the sinoatrial node (SAN) is, to date, unresolved. Here we show that disruption of the gene coding for $Ca_v3.1/\alpha_{1G}$ T-type calcium channels (*cacna1g*) abolishes T-type calcium current ($I_{Ca,T}$) in isolated cells from the SAN and the atrioventricular node without affecting the L-type Ca^{2+} current ($I_{Ca,L}$). By using telemetric electrocardiograms on unrestrained mice and intracardiac recordings, we find that *cacna1g* inactivation causes bradycardia and delays atrioventricular conduction without affecting the excitability of the right atrium. Consistently, no $I_{Ca,T}$ was detected in right atrium myocytes in both wild-type and $Ca_v3.1^{-/-}$ mice. Furthermore, inactivation of *cacna1g* significantly slowed the intrinsic in vivo heart rate, prolonged the SAN recovery time, and slowed pacemaker activity of individual SAN cells through a reduction of the slope of the diastolic depolarization. Our results demonstrate that $Ca_v3.1$/T-type Ca^{2+} channels contribute to SAN pacemaker activity and atrioventricular conduction. **(*Circ Res*. 2006;98:1422-1430.)**

Key Words: pacemaker activity ■ T-type calcium channel ■ sinoatrial node ■ conduction ■ knockout mice

The initiation of the heartbeat requires coordination between the automaticity of the sinoatrial node (SAN) and excitability of the atrioventricular (AV) conduction tissue: the AV node (AVN) and the His–Purkinje fiber network. SAN automaticity is caused by the presence of the diastolic depolarization.[1] Multiple classes of ionic channels are expressed in the SAN,[1,2] but the precise mechanism initiating the diastolic depolarization has not been entirely elucidated, and the relative contribution of different ionic channels in establishing the heart rate under specific physiological conditions is still a matter of debate.[3–5] Strong functional, pharmacological, and genetic evidence show that the hyperpolarization-activated currents I_f[6,7] and $I_{Ca,L}$[8–10] play major roles in controlling the diastolic depolarization after decaying of the fast component of delayed-rectifier K^+ currents (I_{Kr}). Diastolic release of Ca^{2+} mediated by ryanodine receptors (RyRs) has been indicated as an important mechanism for controlling SAN pacemaking under activation of the β-adrenergic receptor.[11] The SAN also expresses neuronal tetrodotoxin (TTX)-sensitive and cardiac TTX-resistant voltage-dependent Na^+ currents (I_{Na}).[12] TTX-sensitive I_{Na} is involved in SAN pacemaking in the newborn rabbit[13] and in the adult mouse.[12,14] The cardiac TTX-resistant *SCN5A*-mediated I_{Na} is important for conduction from the SAN to the atrium and in intranodal conduction.[15] I_{Na} is also expressed in the rabbit[16] and guinea pig[17] AVN and contributes to the fast AV conduction pathway.[18] Consistently, heterozygous mice lacking *SCN5A* channels have major AV conduction dysfunction.[19]

$I_{Ca,T}$ has also been proposed to contribute to pacemaking in primary SAN[20] as well as in latent pacemaker cells of the right atrium (RA).[21] $I_{Ca,T}$ is expressed in pacemaker cells of mammals, including the rabbit[20] and the mouse.[22] $I_{Ca,T}$ is also expressed in the cardiac conduction system, the rabbit AVN,[18] and in canine Purkinje cells.[23,24] The functional role of $I_{Ca,T}$ in the cardiac primary pacemaker and conduction tissue remains to be elucidated.

Molecular cloning of 3 T-type Ca^{2+} channel pore-forming subunits, namely the $Ca_V3.1/\alpha_{1G}$, $Ca_V3.2/\alpha_{1H}$, and $Ca_V3.3/\alpha_{1I}$

Original received November 5, 2004; resubmission received December 5, 2005; revised resubmission received March 30, 2006; accepted April 27, 2006.

From the Institut de Génomique Fonctionnelle (M.E.M., A.T., B.C., L.M., E.K., A.C.-S., J.N., P.L.), CNRS UMR5203-INSERM U661-Université de Montpellier I–Université de Montpellier II, Département de Physiologie, Montpellier; Institut du Thorax (A.-L.L., K.L.Q., D.E., F.C.), INSERM U533, Faculté de Médecine, Nantes; Cardiovascular Research Center (J.V.), INSERM U689, Université Paris 7-Denis Diderot, Paris, France; and Center for Calcium and Learning (H.-S.S.), Korea Institute of Science and Technology, Cheongryang, Seoul, Republic of Korea.

*Both authors contributed equally to this study.

Correspondence to Dr Matteo Mangoni, Institut de Génomique Fonctionnelle, CNRS UMR5203-INSERM U661, Université de Montpellier I–Université de Montpellier II, Département de Physiologie, 141, rue de la Cardonille, Montpellier cedex 05, F-34094 France. E-mail matteo.mangoni@igf.cnrs.fr

Circulation Research **is available at http://circres.ahajournals.org** **DOI: 10.1161/01.RES.0000225862.14314.49**

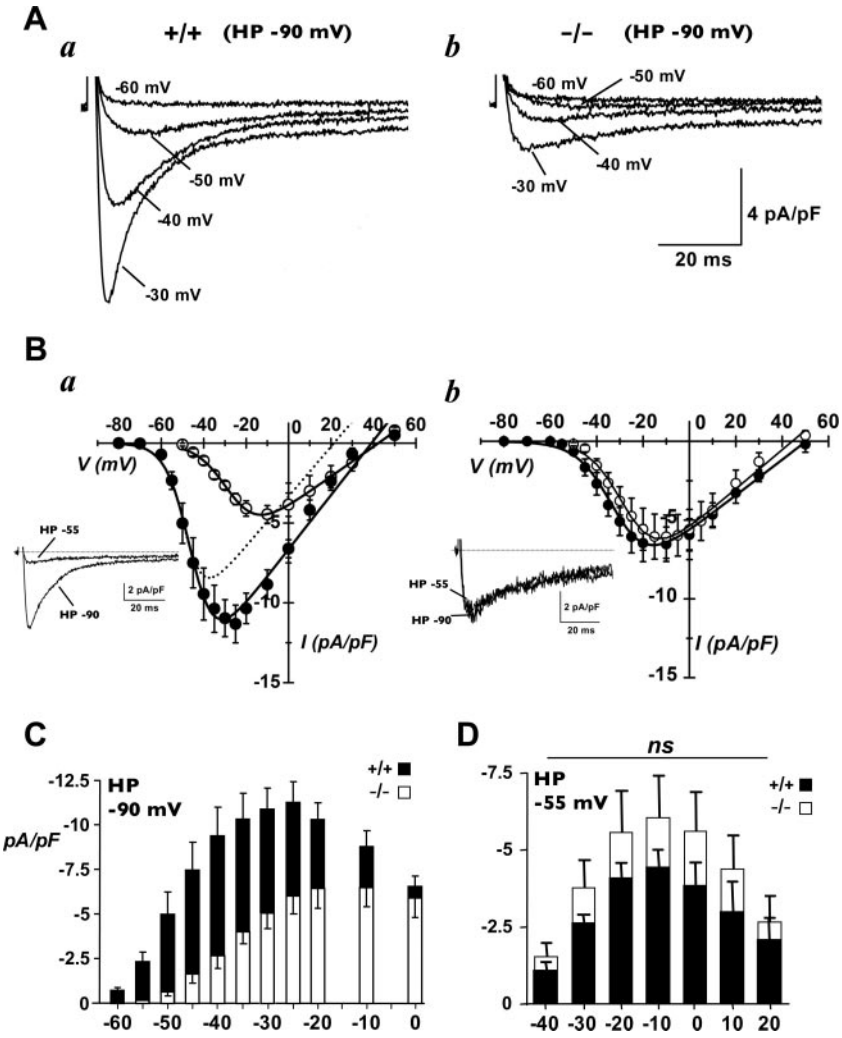

Figure 1. $I_{Ca,T}$ in SAN cells from WT and Ca$_V$3.1$^{-/-}$ mice. A, Typical sample I_{Ca} traces obtained using a HP at −90 mV in a SAN cell from WT (a) and Ca$_V$3.1$^{-/-}$ (b) mice. B, Average I-V curves of the Ca^{2+} current obtained on WT (a) and Ca$_V$3.1$^{-/-}$ (b) SAN cells using a HP at −90 mV (filled symbols) and −55 mV (open symbols). Traces obtained at a test potential of −35 mV, from a HP of −90 and −55 mV, are shown in each inset in a and b, as indicated. The net $I_{Ca,T}$ I-V curve recorded in WT SAN cells is indicated with a dotted line in a and b. C, Histogram showing the relative density of $I_{Ca,T}$ and $I_{Ca,L}$ at different test potentials as indicated. $I_{Ca,T}$ was measured in SAN cells from WT (filled bar), and $I_{Ca,L}$ was measured in SAN cells from Ca$_V$3.1$^{-/-}$ mice (open bar). HP was −90 mV for $I_{Ca,T}$ and $I_{Ca,L}$. D, Density of $I_{Ca,L}$ in SAN cells from WT (open bar) and Ca$_V$3.1$^{-/-}$ (filled bar) mice at different test potentials. ns indicates not significant.

subunits, has fostered investigation of the role of native $I_{Ca,T}$.[25] Here, we describe that Ca$_V$3.1 knockout (Ca$_V$3.1$^{-/-}$) mice lack $I_{Ca,T}$ in both SAN pacemaker and AVN cells and display slowed pacemaker activity and AV conduction. Our results constitute the first direct functional demonstration of the participation of Ca$_V$3.1 channels in pacemaking and cardiac conduction.

Materials and Methods

The generation of the Ca$_V$3.1$^{-/-}$ mouse line was originally described by Kim et al.[26] The experimental procedure for electrophysiological recording of isolated cells from the SAN, the AVN, and the RA is described in the expanded Materials and Methods section in the online data supplement, available at http://circres.ahajournals.org. Detailed procedures for in vivo surface and intracardiac electrocardiograms (ECGs), measurement of blood pressure, RT-PCR, and quantitative RT-PCR experiments (supplemental Figure II) and numerical modeling of pacemaker activity are available in the expanded online Materials and Methods section. Results are presented as the mean±SEM. Statistical significance was assessed by the unpaired Student's *t* test. A value of $P<0.05$ was considered as statistically significant. N indicates the number of mice used and n the number of cells considered.

Results

Ca$_V$3.1$^{-/-}$ SAN Pacemaker Cells Lack $I_{Ca,T}$

Electrophysiological recordings obtained on SAN cells of wild-type (WT) and Ca$_V$3.1$^{-/-}$ animals revealed that $I_{Ca,T}$ related to Ca$_V$3.1 is a major component of the total Ca^{2+} current (I_{Ca}) in SAN cells (Figure 1). Figure 1A shows representative I_{Ca} traces recorded from a holding potential (HP) of −90 mV in WT (Figure 1Aa) and Ca$_V$3.1$^{-/-}$ (Figure 1Ab) SAN cells. No difference in the cell capacitance was detected (see supplementary Figure I). Corresponding current–voltage (I-V) curves are presented in Figure 1B (filled symbols). $I_{Ca,L}$ was measured by applying depolarizing steps from a HP of −55 mV (Figure 1B, open symbols), revealing $I_{Ca,T}$ by subtraction of records from a HP of −55 mV from those obtained from a HP of −90 mV (Figure 1Ba, dotted line). Consistently, switching the HP from −90 to −55 mV significantly shifted I_{Ca} voltage for half activation ($V_{0.5act}$) to more positive values (−45±1 mV; k=5.7±0.6 mV from a HP of −90 mV and −28±1 mV; k=6.3±0.3 mV from a HP of −55 mV, N=9, n=17, $P<0.05$) in all tested cells (n=17), revealing further a $V_{0.5act}$ of −47±1 mV for the net $I_{Ca,T}$ (Figure 1Ba, dotted line). In contrast to WT SAN cells, none

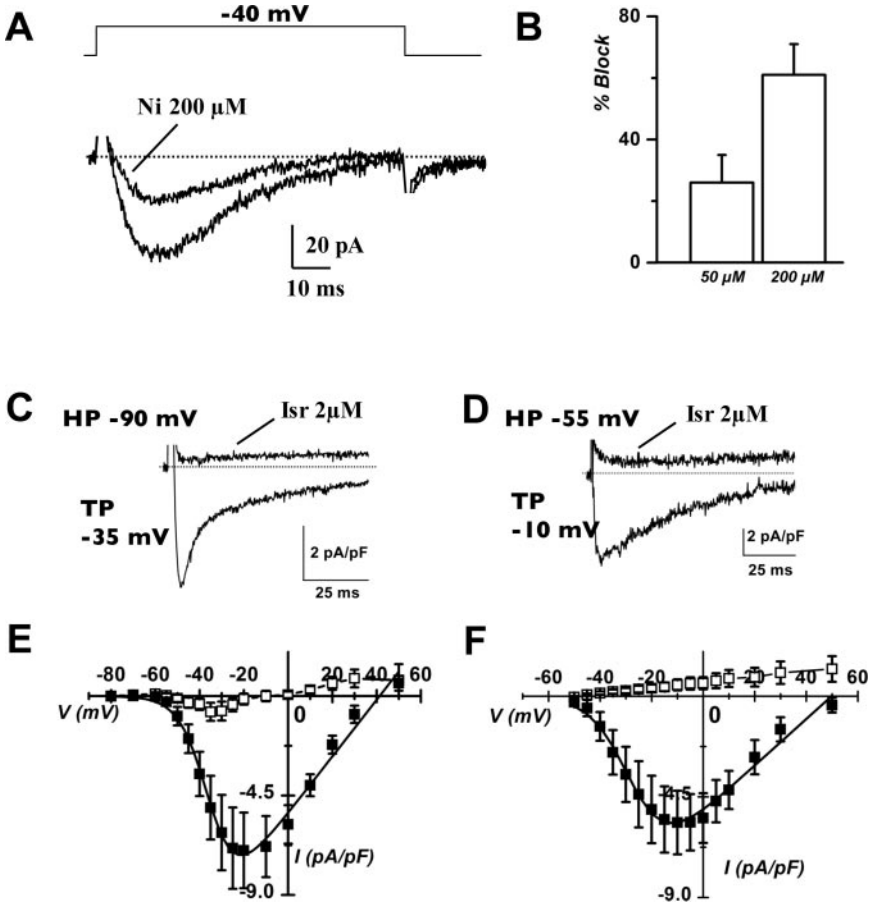

Figure 2. A and B, Sample traces showing partial block of $I_{Ca,T}$ by 200 µmol/L Ni^{2+} in WT SAN cells (A) and histogram of the percentage of inhibition at 50 and 200 µmol/L Ni^{2+} (B). C and D, Isradipine (Isr) block of I_{Ca} in $Ca_V3.1^{-/-}$ SAN cells measured from a HP of −90 mV (C) and −55 mV (D) as indicated. Note that no residual dihydropyridine-resistant $I_{Ca,T}$ is recorded in cells lacking $Ca_V3.1$ channels at the corresponding peak of $I_{Ca,T}$ recorded in WT cells (−35 mV). E and F, Corresponding averaged I-V curves in control conditions (filled boxes) and 2 µmol/L isradipine (open boxes).

of the tested $Ca_V3.1^{-/-}$ cells displayed detectable $I_{Ca,T}$ (Figure 1Bb). Indeed, in $Ca_V3.1^{-/-}$ SAN cells, switching to a HP of −55 mV did not alter significantly voltage dependence of I_{Ca} activation (HP, −90 mV: $V_{0.5act}$=−30±1 mV; k=8.0±1.3 mV, n=14; and HP −55 mV: −28±1 mV; k=6.3±0.3 mV, N=10, n=15, P=NS). Subtraction between traces from HP −90 mV and from HP −55 mV identified no residual $I_{Ca,T}$, because current waveforms displayed slow inactivation kinetics (Figure 1Bb, inset) and no criss-crossing of the current traces. A comparison of the current density values in WT and $Ca_V3.1^{-/-}$ SAN cells at HP −90 mV is shown in Figure 1C (black and white bars, respectively) to estimate the $I_{Ca,T}$ component related to $Ca_V3.1$. At −40 mV, $I_{Ca,T}$ density was 6.8±1.6 pA/pF (+/+, N=9, n=18) and $I_{Ca,L}$ density was 2.6±0.7 pA/pF, (−/−, N=10, n=14). $I_{Ca,L}$ density was not significantly affected by inactivation of $Ca_V3.1$ channels (Figure 1D). Indeed, $I_{Ca,L}$ peak densities at −10 mV (HP, −55 mV) were 6.0±1.6 pA/pF, N=9, n=15; and 4.5±0.6 pA/pF, N=10, n=11 in $Ca_V3.1^{-/-}$ and WT SAN cells, respectively. Taken together, these data showed that inactivation of $Ca_V3.1$ channels abolished $I_{Ca,T}$ and had no significant effect on $I_{Ca,L}$ in SAN cells.

To determine whether the pharmacological sensitivity of the SAN $I_{Ca,T}$ is consistent with the expression of the $Ca_V3.1$ subunit, we tested its sensitivity to Ni^{2+} ions (Figure 2A and 2B). Application of Ni^{2+} concentrations of 50 and 200 µmol/L inhibited 26±9% (N=2, n=4) and 61±10% (n=9) of $I_{Ca,T}$, respectively. Because the IC_{50} values for Ni^{2+} on recombinant $Ca_V3.1$ and $Ca_V3.2$ T-type channels are in the range of 100 to 200 µmol/L and 5 to 10 µmol/L, respectively,[27] these results indicate that $I_{Ca,T}$ in mouse adult SAN cells is generated by the $Ca_V3.1$ subunit. Consistent with these findings, real-time RT-PCR experiments showed that the $Ca_V3.1$ subunit is the predominant T-type Ca^{2+} channel isotype in the SAN of the adult mouse (supplemental Figure II). Furthermore, application of 2 µmol/L of the 1,4-dihydropyridine $I_{Ca,L}$ blocker isradipine on $Ca_V3.1^{-/-}$ SAN cells blocked I_{Ca} by 93±4% (N=5, n=7, Figure 2C and 2E) from a HP of −90 mV and by 100% from a HP of −55 mV (N=5, n=8, Figure 2D and 2F). Such a sensitivity to isradipine further confirmed that the remaining I_{Ca} in SAN cells from $Ca_V3.1^{-/-}$ mice was $I_{Ca,L}$.

Sedated $Ca_V3.1^{-/-}$ Mice Have Intrinsic Slower Heart Rate and Prolonged AV Conduction

We next performed surface ECG recordings on sedated WT and $Ca_V3.1^{-/-}$ mice (Figure 3). Because the heart rate is highly regulated by the balance between the sympathetic and vagal input, which depends on the levels of stress and anesthesia, ECGs were also recorded after injection of propranolol and atropine to block the autonomic nervous system (ANS).[28] Recording examples collected from WT (+/+) and $Ca_V3.1^{-/-}$ (−/−) mice before and after the ANS block are presented in Figure 3A. The loss of the $Ca_V3.1$ subunit induced a significant (9%) prolongation of the atrioventricular conduction (PQ interval) under baseline conditions (34±1

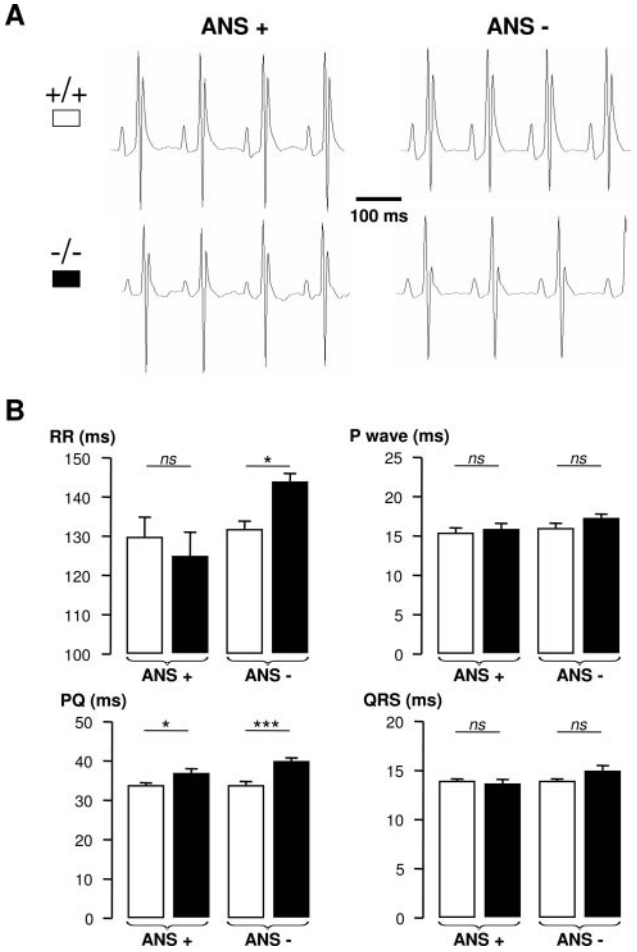

Figure 3. Surface ECGs obtained on sedated WT (+/+) and Ca$_V$3.1$^{-/-}$ (−/−) mice. A, Representative lead I ECG traces obtained from WT and Ca$_V$3.1$^{-/-}$ under baseline conditions (ANS+) (left panels) and after injection of atropine and propranolol to block the ANS (ANS−) (right panels). B, Histograms of the average RR interval, P wave duration, PQ interval, and QRS interval, respectively, obtained from WT (open bars) and Ca$_V$3.1$^{-/-}$ (filled bars) mice, before (ANS+) and after (ANS−) blockade of the ANS.

ms, N=11, and 37±1 ms, N=12 for WT and Ca$_V$3.1$^{-/-}$ mice, respectively; $P<0.05$). The heart beat (RR interval), P wave duration, and QRS interval (Figure 3B), as well as the QTc interval (data not shown; 62±1 ms and 61±1 ms for WT and Ca$_V$3.1$^{-/-}$ mice, respectively; $P>0.05$), were not significantly modified. In conditions of ANS block, the intrinsic heart rate was significantly slowed by ≈10%. Indeed, the RR interval was significantly longer in Ca$_V$3.1$^{-/-}$ mice than in WT animals (144±2 ms and 132±2 ms, respectively; $P<0.05$; Figure 3B). The PQ interval was also markedly prolonged (34±1 ms and 40±1 ms in WT and Ca$_V$3.1$^{-/-}$ animals, respectively; $P<0.001$; Figure 4B). The other ECG parameters were not significantly modified.

SAN Cells From Ca$_V$3.1$^{-/-}$ Mice Display Slowed Pacemaker Activity

The spontaneous activity of isolated SAN cells was studied to evaluate whether the slowing of the intrinsic heart rate observed in vivo in Ca$_V$3.1$^{-/-}$ mice was associated with dysfunction of SAN cell automaticity. Representative recordings obtained on WT and Ca$_V$3.1$^{-/-}$ SAN cells are presented in Figure 4A (upper and lower traces, respectively). Analysis of these recordings showed that inactivation of *cacna1g* gene resulted in a 37% slowing of the cellular beating rate (163±13 bpm, N=4, n=15 in Ca$_V$3.1$^{-/-}$, and 234±19 bpm, N=5, n=14 in SAN cells from WT mice; $P<0.01$; Figure 4B). Slowing of cellular pacemaking was accompanied by a reduction of the diastolic depolarization slope of ≈44% (Figure 4C). No significant changes in the maximum diastolic potential (MDP) and the voltage threshold of the action potential upstroke (E_{th}) were observed (MDP: −56.9±1.3 mV in WT, n=15, and −58.2±1.4 mV for Ca$_V$3.1$^{-/-}$ SAN cells, n=14; E_{th}: −45±1.3 mV in WT and −43±1.4 mV in Ca$_V$3.1$^{-/-}$ SAN cells; Figure 4D). Also, the action potential duration (147±15 and 141±10 ms for Ca$_V$3.1$^{-/-}$ and WT SAN cells, respectively; Figure 4E) and the action potential amplitude (APA) (92±8 and 90±8 mV for Ca$_V$3.1$^{-/-}$ and WT SAN cells, respectively; not shown) were comparable in SAN cells from WT and Ca$_V$3.1$^{-/-}$ mice.

Intracardiac Electrophysiology Study of Ca$_V$3.1$^{-/-}$ Mice

The AV conduction delay in mice lacking Ca$_V$3.1 channels was measured under baseline intracardiac recording conditions. Eight of 10 WT and 7 of 9 Ca$_V$3.1$^{-/-}$ mice had a distinctly visible His-bundle electrogram (Figure 5A). In this group of animals, atrial-His (AH) conduction times were significantly longer in Ca$_V$3.1$^{-/-}$ mice (31±1 ms) than in WT animals (25±1 ms; $P<0.001$; Figure 5B). However, His-ventricle (HV) intervals were comparable (11±1 and 10±1 ms for WT and Ca$_V$3.1$^{-/-}$ mice, respectively; $P>0.05$). Effective refractory periods at the atrial (AERP), atrioventricular (AVERP), and ventricular (VERP) levels were investigated at a basic cycle length of 100 ms (Figure 5C). AERP and VERP were not significantly different between WT and Ca$_V$3.1$^{-/-}$ mice. In contrast, the AVERP was significantly longer in Ca$_V$3.1$^{-/-}$ mice (58±6 ms; N=8) than in WT animals (44±2 ms; N=10; $P<0.05$). Decremental atrial pacing revealed that Wenckebach cycle length was significantly longer in Ca$_V$3.1$^{-/-}$ mice than in WT mice (85±5 ms and 67±2 ms, respectively; $P<0.01$; Figure 5C). Atrial pacing confirmed SAN dysfunction. Indeed, the corrected SAN recovery time (cSNRT) was longer in Ca$_V$3.1$^{-/-}$ mice than in WT mice (31±5 in Ca$_V$3.1$^{-/-}$ and 17±2 ms in WT mice $P<0.05$; n=7 and 9, respectively).

AVN Cells From Ca$_V$3.1$^{-/-}$ Mice Lack $I_{Ca,T}$

We then tested whether dysfunction of AV conduction observed on inactivation of Ca$_V$3.1 channels was associated with downregulation of $I_{Ca,T}$ in the AVN. $I_{Ca,T}$ and $I_{Ca,L}$ were recorded in isolated AVN cells using the same recording protocols as for SAN cells (Figure 6). $I_{Ca,T}$ was found in all the WT AVN cells investigated (Figure 6A). Indeed, switching the HP from −90 to −60 mV significantly shifted the $V_{0.5act}$ of the total I_{Ca} from −34±0.7 to −23±0.8 mV (n=7, $P<0.05$). In contrast, no $I_{Ca,T}$ could be recorded in Ca$_V$3.1$^{-/-}$ AVN cells (Figure 6Ab), and switching the HP from −90 to −60 mV did not shift the $V_{0.5act}$ value (−25±1.3 mV to

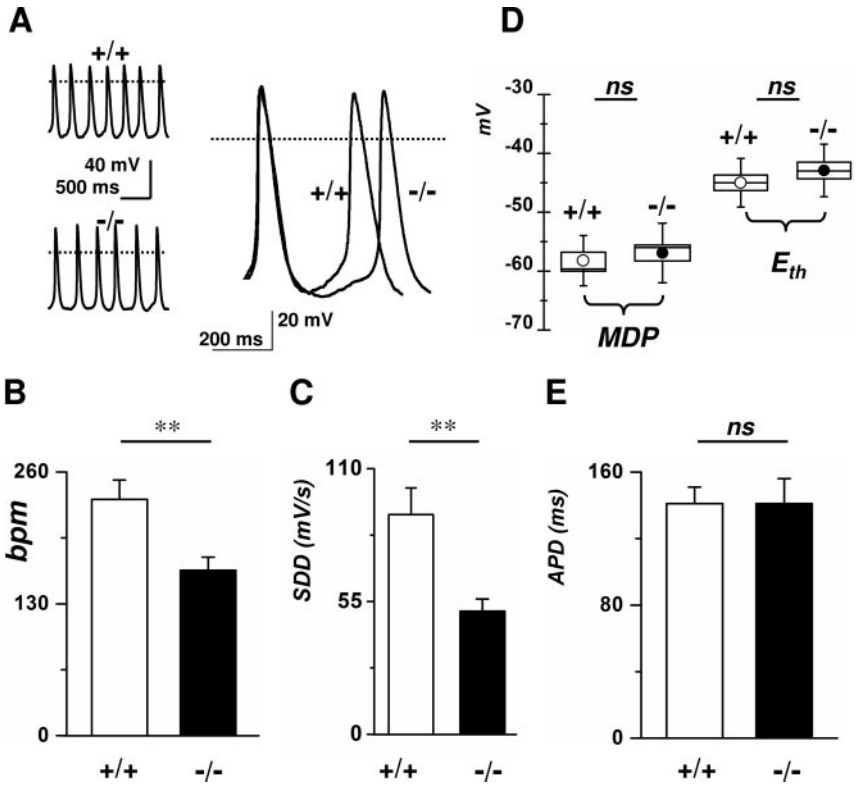

Figure 4. Pacemaker activity of isolated WT (+/+) and $Ca_v3.1^{-/-}$ (−/−) SAN cells. A, Representative sweeps of spontaneous action potentials obtained from SAN cells from WT (upper left trace) and $Ca_V3.1^{-/-}$ mice (lower left trace). Superimposition of typical action potentials from a WT (+/+) and from $Ca_V3.1^{-/-}$ SAN cell (−/−) is shown in phase in the right panel. B and C, Histograms of the average bpm value (B) and the slope of the diastolic depolarization (SDD) (C) SAN cells. D, Box histograms showing the average MDP and the E_{th} in SAN cells from WT (+/+) (open circles) and $Ca_V3.1^{-/-}$ (−/−) (filled circles). Corresponding 25th and 75th percentile define the box. E, Action potential duration (APD) measured in WT and $Ca_V3.1^{-/-}$ SAN cells.

−27±0.8 mV, respectively; P=NS; Figure 6Bb). The peak density of the residual I_{Ca} measured from a HP of −60 mV in AVN cells was not altered by inactivation of $Ca_v3.1$ channels (4.1±0.5 pA/pF, N=5, n=7 in WT and 4.6±0.7 pA/pF, N=4, n=7 in $Ca_v3.1^{-/-}$; P=NS). In addition, no $I_{Ca,T}$ could be detected in isolated cells from the RA of WT adult mice (Figure 6C and 6D), because switching the HP from −100 to −50 mV produced no change both in the $V_{0.5act}$ (−16±2 and −17±1 mV, N=3, n=8, P=NS; Figure 6D) and in the peak density (6.9±1.5 and 7±1 pA/pF, N=3, n=8, P=NS; Figure 6C).

Bradycardia in Conscious Unrestrained $Ca_V3.1^{-/-}$ Mice

Both the heart rate and the AV conduction were altered in freely moving $Ca_V3.1^{-/-}$ mice (Figure 7A and 7B and the Table). The mean heart rate was significantly slowed in $Ca_V3.1^{-/-}$ mice, when considering a 24-hour period or during the day and night periods (Figure 7B and the Table). The maximum cardiac frequency during short periods of activity (40 seconds) was unchanged (Table), suggesting that activation of other ionic channels involved in SAN automaticity can compensate for the lack of $I_{Ca,T}$ during strong activation of the sympathetic nervous system. Spectral analysis of RR signals in the frequency domain revealed no differences between the 2 groups of mice. Total spectral power, ultralow (ULF), very-low (VLF), low (LF), and high (HF) frequencies were not significantly modified between WT and $Ca_V3.1^{-/-}$ mice (Figure 7C, data not shown for ULF and VLF), indicating that the degree of autonomic regulation of heart rate was not altered in $Ca_V3.1^{-/-}$ mice.

Telemetric recordings also confirmed the prolongation of the PQ interval in $Cav3.1^{-/-}$ mice (Table), demonstrating that the propagation of the heartbeat through the AV conduction system was delayed in $Ca_V3.1^{-/-}$ mice. This effect was independent from the heart rate because measurements were performed at comparable heart rates (600 bpm; cycle length of 100 ms). In contrast, the atrial conduction (as assessed by the P wave duration), the ventricular conduction (QRS interval), and ventricular repolarization (QT interval) were unchanged (Table). In addition, we did not find evidence for cardiac arrhythmias in $Ca_V3.1^{-/-}$ mice. Also, no significant difference in the systolic, diastolic, and mean arterial pressure (60±8 mm Hg, N=8 in WT and 72±5 mm Hg, N=8 in $Ca_v3.1^{-/-}$ mice; P=NS) was observed between the 2 mouse strains (Figure 7D).

Discussion

The major finding of this study is that genetic inactivation of the $Ca_V3.1/\alpha_{1G}$ T-type Ca^{2+} channels in mice results in a significant slowing of the heart rate and AV conduction. Downregulation of $I_{Ca,T}$ in both SAN and AVN cells of $Ca_V3.1^{-/-}$ animals is documented, accounting for this in vivo phenotype. The lack of $Ca_v3.1$ channels in isolated SAN cells induces slowing of pacemaker activity through a reduction of the slope of the diastolic depolarization. Our study provides novel and compelling genetic evidence for a direct contribution of $Ca_v3.1$ channels in the setting of the mammalian cardiac impulse generation and propagation by contributing to both the diastolic depolarization in the SAN and impulse conduction through the AVN.

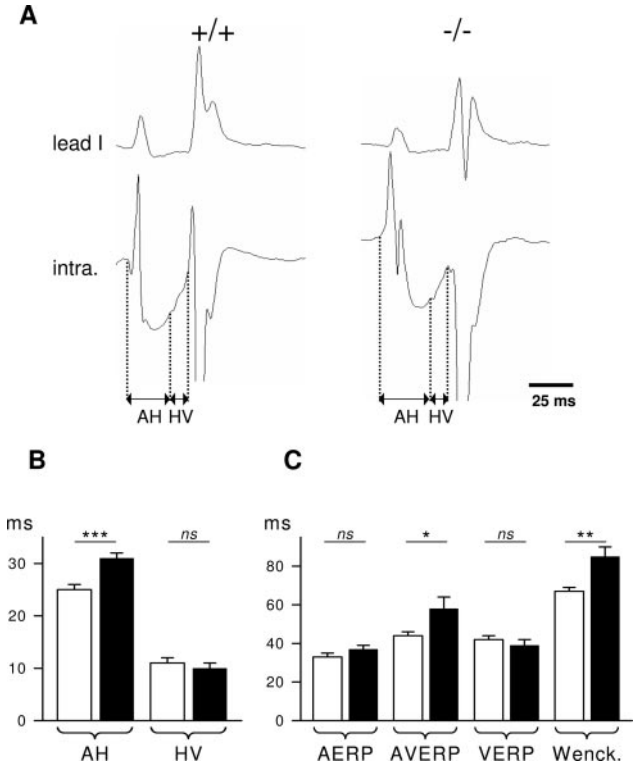

Figure 5. Cardiac electrophysiology studies in anesthetized WT (+/+) and Ca$_V$3.1$^{-/-}$ (−/−) mice. A, Representative surface lead I ECG and intracardiac (intra.) recordings under baseline conditions. B, Histograms of the average AH and HV intervals measured in baseline conditions in WT (open bars; N=8) and Ca$_V$3.1$^{-/-}$ (filled bars; N=7) mice. RR intervals were 111±3 and 122±4 ms for WT and Ca$_V$3.1$^{-/-}$ mice, respectively ($P<0.05$). C, Histograms of the average atrial effective refractory period (AERP), atrioventricular ERP (AVERP), ventricular ERP (VERP), and AV Wenckebach cycle length (Wenck.) in WT (open bars; N=9 to 10) and Ca$_V$3.1$^{-/-}$ (filled bars; N=6 to 8) mice.

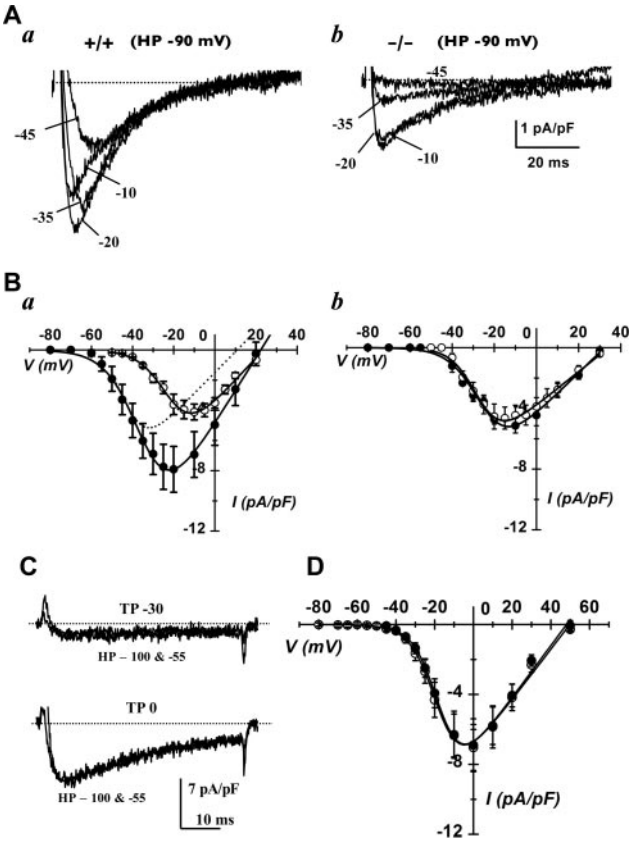

Figure 6. Recordings of I_{Ca} in isolated AVN and RA cells from WT and Ca$_V$3.1$^{-/-}$ mice. A, Sample I_{Ca} traces obtained using a HP at −90 mV in a AVN cell from WT (a) and Ca$_V$3.1$^{-/-}$ (b) mice. B, I-V curves of I_{Ca} obtained on WT (a) and Ca$_V$3.1$^{-/-}$ (b) SAN cells using a HP at −90 mV (filled symbols) and −60 mV (open symbols). The I-V curve of $I_{Ca,T}$ calculated by subtracting records at HP of −60 mV from that at HP of −90 mV are shown as a dotted line. C and D, Lack of $I_{Ca,T}$ in RA cells from WT mice. Sample traces recorded from a HP of −100 mV at test potential (TP) values of −30 and 0 mV are shown in C; Averaged I-V curves marked as in (B) are shown in D.

$I_{Ca,T}$ in SAN and AVN Cells Following Inactivation of Ca$_V$3.1 Channels

A striking observation of this study is that $I_{Ca,T}$ in the mouse SAN is predominantly generated by the Ca$_V$3.1 subunit because we found no evidence for a residual $I_{Ca,T}$ in Ca$_V$3.1$^{-/-}$ mice in both SAN (Figure 1) and AVN cells (Figure 6). The low sensitivity of SAN $I_{Ca,T}$ to Ni^{2+} is consistent with that observed on recombinant Ca$_V$3.1-mediated $I_{Ca,T}$.[27] Also consistent with our general findings is the recent observation that Ca$_V$3.2$^{-/-}$ mice showed no ECG alterations.[29] Inactivation of Ca$_V$3.1 channels did not significantly modify the expression of $I_{Ca,L}$ in Ca$_V$3.1$^{-/-}$ in both SAN and AVN cells. Our data show, therefore, that expression of Ca$_V$3.2, Ca$_V$1.3, and Ca$_V$1.2 subunits do not compensate for the lack of Ca$_V$3.1 channels in Ca$_V$3.1$^{-/-}$ mice.

Bradycardia and Atrioventricular Dysfunction in Ca$_V$3.1$^{-/-}$ Mice

ECGs and intracardiac recordings document both bradycardia and slowing of the atrioventricular conduction in Ca$_V$3.1$^{-/-}$ mice. Several lines of evidence indicate that bradycardia is attributable to slowing of the pacemaker activity in the SAN. First, bradycardia was evident in sedated mice under pharmacological blockade of the ANS input for heart rates that were comparable with the mean heart rate observed in freely moving mice. Second, slowing of the heart rate was observed in freely moving mice in the absence of a significant change both in the heart rate variability profile and in the arterial blood pressure, thus arguing against the hypothesis that bradycardia would be caused by dysfunction in the autonomic regulation of the heart rate or could be secondary to a change in the control of the vascular tone. The prolongation of the SAN recovery time also indicates dysfunction in SAN automaticity. Finally, the slowing of pacemaker activity observed in isolated SAN pacemaker cells of Ca$_V$3.1$^{-/-}$ mice is consistent with bradycardia being attributable to the lack of $I_{Ca,T}$ in the SAN. The reduction of the mean heart rate measured on freely moving Ca$_V$3.1$^{-/-}$ mice is moderate, compared with the slowing of the cycle length in isolated pacemaker cells (10% in freely moving mice and 37% in isolated cells). This difference can be caused by the compensatory adrenergic tone in vivo, which stimulates ionic mechanisms involved in pacemaking, such as Ca$_V$1.3-mediated $I_{Ca,L}$[9,10] and I_f[6] and RyR-dependent diastolic release of Ca^{2+}.[11] The observation that the maximal heart rate is comparable in WT and

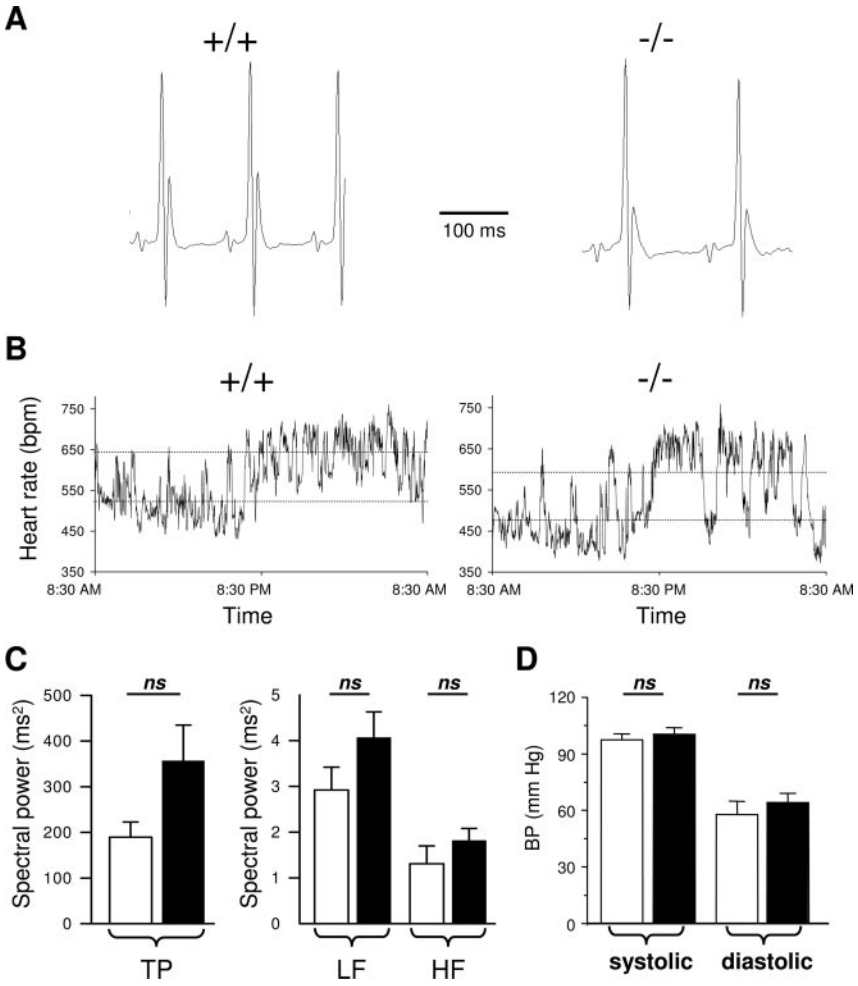

Figure 7. Twenty-four-hour telemetric ECG recordings in conscious unrestrained WT (+/+) and $Ca_V3.1^{-/-}$ (−/−) mice. A, Representative ECG recordings obtained on WT and $Ca_V3.1^{-/-}$ animals during daytime. B, Examples of circadian variation of heart rate (in bpm) in WT and $Ca_V3.1^{-/-}$ mice over a 24-hour period. Dashed lines indicate mean day and night heart rates. C, Spectral analysis of heart rate variability. Results are illustrated for total power spectra (0 to 3.2 Hz) and specific frequency bands, ie, low frequency (LF) (0.32 to 1.2 Hz) and high frequency (HF) (1.2 to 3.2 Hz). Note that during the study period, heart rate was significantly slowed in $Ca_V3.1^{-/-}$ mice (455±13 bpm and 515±10 bpm for $Ca_V3.1^{-/-}$ and WT mice, respectively; $P<0.005$). TP indicates, test potential. D, Measurements of the systolic and diastolic blood pressure in WT (open bars; n=8) and $Ca_V3.1^{-/-}$ (filled bars; n=8) mice.

$Ca_v3.1^{-/-}$ mice is consistent with this hypothesis. Comparison of mice lacking $Ca_v1.3$[9] and $Ca_v3.1$ channels (this study) indicate that $I_{Ca,L}$ and $I_{Ca,T}$ play distinct roles in pacemaker activity in vivo. Indeed, knockout of $Ca_v1.3$ channels reduces the basal and intrinsic heart rate in sedated conditions by approximately 20% and 60%, respectively,[9] compared with the 10% reduction observed in mice lacking $Ca_v3.1$ channels in both freely moving and block of ANS conditions. These observations suggest that $Ca_v3.1$ channels contribute to the setting of the basal heart rate but have less impact on the dynamic regulation of pacemaker activity by the ANS. The lack of a significant change in the variability of the RR intervals in $Ca_v3.1$ mice is consistent with this hypothesis.

We report that the slowing of the AV conduction in $Ca_v3.1^{-/-}$ mice is caused by dysfunction in the excitability of the AVN. Indeed, intracardiac recordings show a delay in the AH conduction time and AVERP, in the absence of a prolongation of the P wave, which indicates similar conduction velocities in atria from WT and $Ca_v3.1^{-/-}$ mice. Consistently with ECGs and intracardiac recordings, we found no $I_{Ca,T}$ in atrial myocytes from WT mice. Also, AVN cells display $I_{Ca,T}$ related to $Ca_V3.1$ channels because it was no longer detectable in $Ca_V3.1^{-/-}$ mice. We did not find significant changes in the HV, QRS, and QT intervals (see Figures 3 and 5 and supplemental Figure III), indicating that the lack of $Ca_v3.1$ channels does not affect conduction through the His–Purkinje fiber network or the ventricular muscle. This phenotype differs from that of *SCN5A*$^{+/-}$ mice,[19] which shows prominent alteration of the P wave and the QRS complex duration,[30] stressing the importance of the cardiac

Telemetric ECG Parameters in Freely Moving WT and $Ca_V3.1^{-/-}$ Mice

	Heart Rate (bpm)					ECG Parameters			
	Mean HR (24 hours)	Daytime Mean HR	Nighttime Mean HR	HR Minimum (40 seconds)	HR Maximum (40 seconds)	P Wave Duration (ms)	PQ Interval (ms)	QRS Interval (ms)	QT Interval (ms)
WT	578±14	526±11	630±18	404±8	775±10	13±1	32±1	12±1	56±2
$Ca_V3.1^{-/-}$	524±11	476±13	571±12	358±18	742±15	14±1	35±0	12±0	52±2
P	0.012	0.015	0.022	0.039	NS	NS	0.004	NS	NS

ECG parameters were set at a cycle length of 100 ms. WT, N=6; $Ca_V3.1^{-/-}$, N=6. HR indicates heart rate.

I_{Na} in intraatrial and His–Purkinje conduction. Also in contrast with *SCN5A*$^{+/-}$,[19] Ca$_v$3.1$^{-/-}$ mice do not present ventricular tachiarrhythmias. This SCN5A-mediated I_{Na} can possibly compensate for the lack of $I_{Ca,T}$ in the His–Purkinje system.

Pacemaking in Ca$_v$3.1$^{-/-}$ Mice

We describe that inactivation of Ca$_V$3.1 channels significantly prolongs the pacemaker cycle length in isolated SAN cells by reducing the slope of the diastolic depolarization, demonstrating the involvement of Ca$_v$3.1-mediated $I_{Ca,T}$ in the setting of the diastolic depolarization in mouse SAN cells. In an attempt to compare the physiological roles of Ca$_v$3.1-mediated $I_{Ca,T}$ with that of Ca$_v$1.3-mediated $I_{Ca,L}$ and I_{Na}, we have developed a numerical model of mouse SAN electrophysiology based on previous studies on mouse SAN pacemaking in normal and genetically modified mouse strains (see supplemental Figures IV and V). Our numerical simulations indicate that Ca$_v$3.1 channels contribute to pacemaking by activating during the diastolic depolarization for more negative voltages than TTX-sensitive I_{Na} and Ca$_v$1.3-mediated $I_{Ca,L}$ (see supplemental Figure VB and VE). As a consequence, Ca$_v$3.1 channels can accelerate the diastolic depolarization rate in a voltage range in which I_{Na} is still not activated. This property can explain, at least in part, how Ca$_v$3.1 channels can contribute to pacemaking in spite of their relatively low availability at SAN diastolic potentials. An expanded discussion about the development, the features and limitations of our numerical model, and the physiological significance of Ca$_v$3.1-mediated $I_{Ca,T}$ compared with that of $I_{Ca,L}$ and I_{Na} is available in the online data supplement.

Conclusion

In conclusion, our study demonstrates that Ca$_V$3.1 channels contribute to the heartbeat by influencing pacemaking and the AV conduction. To date, the presence of T-type channels in human heart is poorly documented. Molecular analyses, such as dot blots and Northern blots of human heart mRNAs, have identified transcripts for Ca$_V$3.1 and Ca$_V$3.2.[31,32] T-type channels may play a role in the human SAN and the conduction system. For instance, the causality between congenital heart block induced by maternal autoantibodies against T-type channels and children showing SAN bradycardia and atrioventricular block has recently been documented.[33] There is growing evidence that T-type channels may constitute a promising pharmacological target for the treatment of human diseases, such as epilepsy and chronic pain.[34] From our observations, T-type channel inhibition would have no deleterious consequences in cardiac physiology. It is, therefore, tempting to speculate that selective blockers of Ca$_V$3.1 channels may hold promise for the therapeutic management of the cardiac diseases that require moderate heart rate reduction, such as cardiac ischemia and coronary heart disease.

Acknowledgments

This work was supported by the Association Française Contre les Myopathies, the Action Concertée Incitative (Developmental Biology and Integrative Physiology) of the French Ministry for Education, the Fondation de France, and the Chemoinformatics Program of Korean Institute of Science and Technology, Korea. A.T. is supported by a fellowship from the CNRS Lebanon. We are grateful to Patrick Atger for excellent technical assistance.

References

1. Irisawa H, Brown HF, Giles W. Cardiac pacemaking in the sinoatrial node. *Physiol Rev*. 1993;73:197–227.
2. Boyett MR, Honjo H, Kodama I. The sinoatrial node, a heterogeneous pacemaker structure. *Cardiovasc Res*. 2000;47:658–687.
3. Difrancesco D. Serious workings of the funny current. *Prog Biophys Mol Biol*. 2006;90:13–25.
4. Lakatta EG, Maltsev VA, Bogdanov KY, Stern MD, Vinogradova TM. Cyclic variation of intracellular calcium: a critical factor for cardiac pacemaker cell dominance. *Circ Res*. 2003;92:e45–e50.
5. Honjo H, Inada S, Lancaster MK, Yamamoto M, Niwa R, Jones SA, Shibata N, Mitsui K, Horiuchi T, Kamiya K, Kodama I, Boyett MR. Sarcoplasmic reticulum Ca^{2+} release is not a dominating factor in sinoatrial node pacemaker activity. *Circ Res*. 2003;92:e41–e44.
6. Baruscotti M, Bucchi A, Difrancesco D. Physiology and pharmacology of the cardiac pacemaker ("funny") current. *Pharmacol Ther*. 2005;107:59–79.
7. Stieber J, Herrmann S, Feil S, Loster J, Feil R, Biel M, Hofmann F, Ludwig A. The hyperpolarization-activated channel HCN4 is required for the generation of pacemaker action potentials in the embryonic heart. *Proc Natl Acad Sci U S A*. 2003;100:15235–15240.
8. Verheijck EE, van Ginneken AC, Wilders R, Bouman LN. Contribution of L-type Ca^{2+} current to electrical activity in sinoatrial nodal myocytes of rabbits. *Am J Physiol*. 1999;276:H1064–H1077.
9. Zhang Z, Xu Y, Song H, Rodriguez J, Tuteja D, Namkung Y, Shin HS, Chiamvimonvat N. Functional Roles of Ca$_v$1.3 α_{1D} calcium channel in sinoatrial nodes: insight gained using gene-targeted null mutant mice. *Circ Res*. 2002;90:981–987.
10. Mangoni ME, Couette B, Bourinet E, Platzer J, Reimer D, Striessnig J, Nargeot J. Functional role of L-type Cav1.3 Ca^{2+} channels in cardiac pacemaker activity. *Proc Natl Acad Sci U S A*. 2003;100:5543–5548.
11. Vinogradova TM, Bogdanov KY, Lakatta EG. beta-Adrenergic stimulation modulates ryanodine receptor Ca^{2+} release during diastolic depolarization to accelerate pacemaker activity in rabbit sinoatrial nodal cells. *Circ Res*. 2002;90:73–79.
12. Lei M, Jones SA, Liu J, Lancaster MK, Fung SS, Dobrzynski H, Camelliti P, Maier SK, Noble D, Boyett MR. Requirement of neuronal- and cardiac-type sodium channels for murine sinoatrial node pacemaking. *J Physiol*. 2004;559:835–848.
13. Baruscotti M, DiFrancesco D, Robinson RB. A TTX-sensitive inward sodium current contributes to spontaneous activity in newborn rabbit sino-atrial node cells. *J Physiol*. 1996;492:21–30.
14. Maier SK, Westenbroek RE, Yamanushi TT, Dobrzynski H, Boyett MR, Catterall WA, Scheuer T. An unexpected requirement for brain-type sodium channels for control of heart rate in the mouse sinoatrial node. *Proc Natl Acad Sci U S A*. 2003;100:3507–3512.
15. Lei M, Goddard C, Liu J, Leoni AL, Royer A, Fung SS, Xiao G, Ma A, Zhang H, Charpentier F, Vandenberg JI, Colledge WH, Grace AA, Huang CL. Sinus node dysfunction following targeted disruption of the murine cardiac sodium channel gene Scn5a. *J Physiol*. 2005;567:387–400.
16. Munk AA, Adjemian RA, Zhao J, Ogbaghebriel A, Shrier A. Electrophysiological properties of morphologically distinct cells isolated from the rabbit atrioventricular node. *J Physiol*. 1996;493:801–818.
17. Yuill KH, Hancox JC. Characteristics of single cells isolated from the atrioventricular node of the adult guinea-pig heart. *Pflugers Arch*. 2002;445:311–320.
18. Efimov IR, Nikolski VP, Rothenberg F, Greener ID, Li J, Dobrzynski H, Boyett M. Structure-function relationship in the AV junction. *Anat Rec A Discov Mol Cell Evol Biol*. 2004;280:952–965.
19. Papadatos GA, Wallerstein PM, Head CE, Ratcliff R, Brady PA, Benndorf K, Saumarez RC, Trezise AE, Huang CL, Vandenberg JI, Colledge WH, Grace AA. Slowed conduction and ventricular tachycardia after targeted disruption of the cardiac sodium channel gene Scn5a. *Proc Natl Acad Sci U S A*. 2002;99:6210–6215.
20. Hagiwara N, Irisawa H, Kameyama M. Contribution of two types of calcium currents to the pacemaker potentials of rabbit sino-atrial node cells. *J Physiol*. 1988;395:233–253.
21. Huser J, Blatter LA, Lipsius SL. Intracellular Ca^{2+} release contributes to automaticity in cat atrial pacemaker cells. *J Physiol*. 2000;524:415–422.

22. Mangoni ME, Nargeot J. Properties of the hyperpolarization-activated current (I_f) in isolated mouse sino-atrial cells. *Cardiovasc Res*. 2001;52: 51–64.
23. Hirano Y, Fozzard HA, January CT. Characteristics of L- and T-type Ca^{2+} currents in canine cardiac Purkinje cells. *Am J Physiol*. 1989;256: H1478–H1492.
24. Tseng GN, Boyden PA. Multiple types of Ca^{2+} currents in single canine Purkinje cells. *Circ Res*. 1989;65:1735–1750.
25. Perez-Reyes E. Molecular physiology of low-voltage-activated T-type calcium channels. *Physiol Rev*. 2003;83:117–161.
26. Kim D, Song I, Keum S, Lee T, Jeong MJ, Kim SS, McEnery MW, Shin HS. Lack of the burst firing of thalamocortical relay neurons and resistance to absence seizures in mice lacking α_{1G} T-type Ca^{2+} channels. *Neuron*. 2001;31:35–45.
27. Lee JH, Gomora JC, Cribbs LL, Perez-Reyes E. Nickel block of three cloned T-type calcium channels: low concentrations selectively block alpha1H. *Biophys J*. 1999;77:3034–3042.
28. Lande G, Demolombe S, Bammert A, Moorman A, Charpentier F, Escande D. Transgenic mice overexpressing human KvLQT1 dominant-negative isoform. Part II: pharmacological profile. *Cardiovasc Res*. 2001; 50:328–334.
29. Chen CC, Lamping KG, Nuno DW, Barresi R, Prouty SJ, Lavoie JL, Cribbs LL, England SK, Sigmund CD, Weiss RM, Williamson RA, Hill JA, Campbell KP. Abnormal coronary function in mice deficient in α_{1H} T-type Ca^{2+} channels. *Science*. 2003;302:1416–1418.
30. Royer A, van Veen TA, Le Bouter S, Marionneau C, Griol-Charhbili V, Leoni AL, Steenman M, van Rijen HV, Demolombe S, Goddard CA, Richer C, Escoubet B, Jarry-Guichard T, Colledge WH, Gros D, de Bakker JM, Grace AA, Escande D, Charpentier F. Mouse model of SCN5A-linked hereditary Lenegre's disease: age-related conduction slowing and myocardial fibrosis. *Circulation*. 2005;111:1738–1746.
31. Cribbs LL, Lee JH, Yang J, Satin J, Zhang Y, Daud A, Barclay J, Williamson MP, Fox M, Rees M, Perez-Reyes E. Cloning and characterization of alpha1H from human heart, a member of the T-type Ca^{2+} channel gene family. *Circ Res*. 1998;83:103–109.
32. Monteil A, Chemin J, Bourinet E, Mennessier G, Lory P, Nargeot J. Molecular and functional properties of the human α_{1G} subunit that forms T-type calcium channels. *J Biol Chem*. 2000;275:6090–6100.
33. Hu K, Qu Y, Yue Y, Boutjdir M. Functional basis of sinus bradycardia in congenital heart block. *Circ Res*. 2004;94:e32–e38.
34. Birch PJ, Dekker LV, James IF, Southan A, Cronk D. Strategies to identify ion channel modulators: current and novel approaches to target neuropathic pain. *Drug Discov Today*. 2004;9:410–418.